



Zodiacal Light Emission in forthcoming full-sky microwave surveys

M. Maris¹ and C. Burigana²

¹ INAF - Osservatorio Astronomico di Trieste, Via G.B.Tiepolo 11, I-34143, Trieste, Italy
e-mail: maris@oats.inaf.it

² INAF-IASF Bologna, Via Gobetti 101, I-40129, Bologna, Italy e-mail:
burigana@iasfbo.inaf.it

Abstract. In the context of current and future microwave surveys mainly dedicated to the accurate mapping of CMB anisotropy, the Zodiacal Light Emission (ZLE) represents a potential source of foreground. In this contribution we shortly review the current knowledge in the field and describe the fundamental aspects in ZLE modelling. All-sky templates of ZLE suitable for applications in the microwaves are presented. We discuss the new perspectives in the field opened by the new high-sensitivity microwave surveys: the understanding of the SED below 1 THz and refinement of the ZLE geometrical properties. Likely, this will open highlights on the properties of IDPs. A particular attention is devoted to the forthcoming information achievable with PLANCK.

Key words. 1 interplanetary medium 2 (infrared:) solar system 3 (cosmology:) cosmic microwave background

1. Introduction and motivations for this work

The existence of a cloud of Interplanetary Dust Particles (IDPs) is evidenced by the observation of meteors, erosion and microcraterization of surfaces of bodies without atmosphere, hits on spacecrafts and direct collection of grains in the upper atmosphere of the Earth, but the concept of interplanetary dust traces back at least to Giandomenico Cassini, who first interpreted the Zodiacal Light as the scattering of sun-light by such particles. Presently, detections of Zodiacal Light have been reported from the UV (Waller et al. , 1995) down to the far infrared (Fixsen & Dwek , 2002). In

the infrared the thermal emission of IDPs dominates over scattering for wavelengths longer than $3.5 \mu\text{m}$ and the emission is often referred as Zodiacal Light Emission (ZLE).

The Zodiacal Light (and the ZLE) represents an important foreground for surveys dedicated to the large scale distribution of “far” diffused sources, such as those attempting the detection of the extragalactic background in the visible (Bernstein et al. , 2002a,b; Mattila , 2003) or in the infrared (Bock et al. , 2006) where the ZLE is characterized by a smooth, large scale structure, with weak fluctuations below the degree scale (Ábrahám et al. , 1997), and those dedicated to the study of the CMB.

The increasing sensitivity of large scale surveys in the (sub)mm bands, in particular

Send offprint requests to: M. Maris

those dedicated to the study of the Cosmic Microwave Background (CMB), will require a careful separation and subtraction of any source of weak “Galactic” foreground, forcing to consider other sources of Galactic emissions over the traditional ones (synchrotron, Galactic thermal emission, free-free emission). In fact, at frequencies ≈ 10 THz the ZLE dominates the sky emissivity. At frequencies below ≈ 1 THz the ZLE is subdominant compared to the Galaxy, but its surface brightness is still significant Fixsen & Dwek (2002), particularly in regions where the Galactic emission is weak Maris et al. (2006a). In preparing templates of Galactic emission from observations at these frequencies the contamination of ZLE has to be accurately accounted for, since the ability to model and remove the ZLE will fix the final accuracy of the Galactic templates used at lower frequencies to separate the “local” contribution from the cosmological radiation. It is then reasonable to expect that these surveys will provide in the future better and better calibrated full-sky maps leading to the possibility to detect the ZLE even in cases in which its contribution is weak in comparison to other diffuse sources in the sky.

It is important to consider that all-sky surveys require time to be completed and in the while the observer moves sensitively within the IDPs cloud. Consequently, the ZLE depends on the location of the observer, \mathbf{R}_p , within the Solar System and not only on the pointing direction, \mathbf{P} . Then the ZLE behaves as a time-dependent foreground and, when not properly removed, may introduce subtle systematic effects. This means that a proper modeling of ZLE requires a full 3D model of the IDPs cloud. Ideally, a self-consistent dynamical model of the IDPs distribution would be the best choice for a 3D model. Various authors, motivated even by space applications, developed such comprehensive numerical models attempting to integrate all the sources of information, i.e. surveys, shape of Fraunhofer lines in the scattered Sun-light, meteoroid fluxes, impact sensors onboard spacecrafts and Moon microcraterization (Gor’kavyi et al. , 2002; Ishimoto , 2000; Dikarev et al. , 2005, to cite only few). On the other hand, this effort

is made difficult by the complexity of IDPs dynamics which is dominated by collisions, Pointing-Robertson (as other radiative effects), evaporation by solar heating and it is sensitive to the details of the chemical and mineralogical composition of particles. In addition IDPs are depleted in a relatively short time and the IDPs cloud is unstable leading to the problem of what are the sources of dust refilling the cloud. Comets, asteroids, KBO and an incoming flux of interstellar dust are supposed to be sources of IDPs with varying proportions changing the heliocentric distance. A multiplicity of grain populations with varying properties are then contributing to the IDPs complex. Indeed IRAS ¹, ISO ² and COBE ³ surveys revealed a structured system of IDPs clouds in the Solar System. As an example, the recent phenomenological *COBE model* (Kelsall et al. , 1998) splits the IDPs cloud in a *bulk* or *smooth* component, three *bands of dust*, a *circumsolar ring* and a *trailing blob*. A number of *cometary trails* has been also detected in the past by IRAS and ISO.

These considerations motivated our effort to study the ZLE within the forthcoming ESA PLANCK mission (Maris et al. , 2006a,b), as part of a more extended study including other Solar System objects (Cremonese et al. , 2002; Maris et al. , 2003, 2004). In this work we refer to PLANCK as our reference mission. However methods and results can be extended to other (sub)mm forthcoming observatories, for example Herschel ⁴ and ALMA ⁵. A detailed presentation of the ESA PLANCK satellite ⁶, scheduled for launch in 2008, is outside the scope of this work. We remember here that PLANCK is a full-sky surveyor dedicated to CMB and (sub)mm astronomy and represents a third generation mission after COBE and WMAP ⁷. PLANCK is equipped with a 1.5 m Gregorian aplanatic telescope, carrying in the focal surface two in-

¹ <http://lambda.gsfc.nasa.gov/product/iras>

² <http://www.iso.vilspa.esa.es>

³ <http://lambda.gsfc.nasa.gov/product/cobe>

⁴ <http://www.rssd.esa.int/herschel>

⁵ <http://www.alma.nrao.edu>

⁶ <http://www.rssd.esa.int/planck>

⁷ <http://map.gsfc.nasa.gov>

struments covering the frequency bands 30, 44, and 70 GHz - Low Frequency Instrument, LFI - and 100, 143, 217, 353, 545, and 857 GHz - High Frequency Instrument, HFI.

2. Model and extrapolations

As for the Galactic dust contamination, the modeling of the ZLE has to be based on far infrared observations, at least for what concerns the geometrical aspects of the IDPs distribution. Key data for the ZLE below $300 \mu\text{m}$ have been obtained by IRAS Wheelock et al. (1994), COBE Fixsen & Dwek (2002); Kelsall et al. (1998) and ISO Reach et al. (1996, 2003). The starting point for this analysis is the COBE/DIRBE model for the ZLE which describes the expected local 3D emissivity within the IDPs complex Kelsall et al. (1998). In particular, among the various components in which the IDPs are distributed we refer here to the dominant *Smooth* component which accounts for more than 90% of the ZLE. For frequencies $f \lesssim 1$ THz the total brightness of the ZLE integrated along a given line-of-sight is

$$I_f(\mathbf{P}, \mathbf{R}_p) = E_f Z_f(\mathbf{P}, \mathbf{R}_p), \quad (1)$$

where $Z_f(\mathbf{P}, \mathbf{R}_p)$ gives the spatial dependence i.e. the integral along the line-of-sight of the black body emission of IDPs whose temperature and numerical density is assumed to vary with the heliocentric distance. The *Emissivity Factor* E_f is a correction with respect to a pure blackbody emission law, related to the composition and size distribution of dust grains. Following Kelsall et al. (1998) it is assumed $E_f = 1$ for $f = 12$ THz.

In long duration CMB experiments the sky is observed for a set of pointing directions ordered in time according to a certain scanning strategy. In the while the observer is orbiting around the Sun and consequently the ZLE will show seasonal modulations at the level of 5 - 15% Reach (1997) mainly due to the tilt of IDPs cloud over the ecliptic plane. Changes in the spacecraft orbit and/or in the observation epoch will result in different realizations of ZLE sky maps even when the sky is

sampled according to the same scanning strategy. To condensate into a statical map this dynamical information we exploit the cylindrical symmetry of the COBE model. We develop a new method based on series expansions of $Z_f(\mathbf{P}, \mathbf{R}_p)$ about an averaged orbit in the IDPs cloud reference frame. This is equivalent to calculate a kernel map for $Z_f(\mathbf{P}, \mathbf{R}_p)$ which is good for a given “nominal” mission together with coefficients to be used in computing variations of the map for a range of possible realization of the mission Maris et al. (2006a). The method allows to generate both time ordered data streams as time averaged maps saving even a factor ≈ 60 in computing time and may be used to condensate the information of other 3D models over the COBE model Maris et al. (2006a).

The extrapolation of E_f at frequencies below 1 THz is a more delicate problem. COBE/DIRBE measures extend down to $f = 1.2$ THz, which fixes the lowest frequency for which the COBE model provides values of E_f Kelsall et al. (1998). However COBE/FIRAS provides measures of ZLE averaged over the sky and over one year down to $f \approx 0.3$ THz Fixsen & Dwek (2002) but with a not so good sensitivity. We then compare the COBE/DIRBE measures with simulated yearly and full-sky averaged values of $Z_f(\mathbf{P}, \mathbf{R}_p)$ in order to evaluate E_f . In this way we can obtain numerical estimates for these parameters Maris et al. (2006a). Similar results are also obtained directly extrapolating E_f values derived by COBE/DIRBE at $f < 12$ THz down to the required frequencies. These calculations predicts the ZLE to be in the range $(1-6) \times 10^{-1}$ MJy/sr for the 857 GHz frequency channel down to $(0.4 - 2) \times 10^{-2}$ MJy/sr for the 353 GHz frequency channel (Maris et al. , 2006b, see Tab. 1 in this reference for details). Fig. 1 (left panel) shows the surface brightness ratios between the ZLE and the Galaxy (upper region and lines) and between the instrumental noise and the Galaxy (bottom region). In the plot, ideal bands of sky are drawn around minor circles of 85° of radius and 2° of width; an example is drawn in the map of Fig. 1 (right panel). The centers of bands lay on the ecliptic and are drawn for a set of selected eclip-

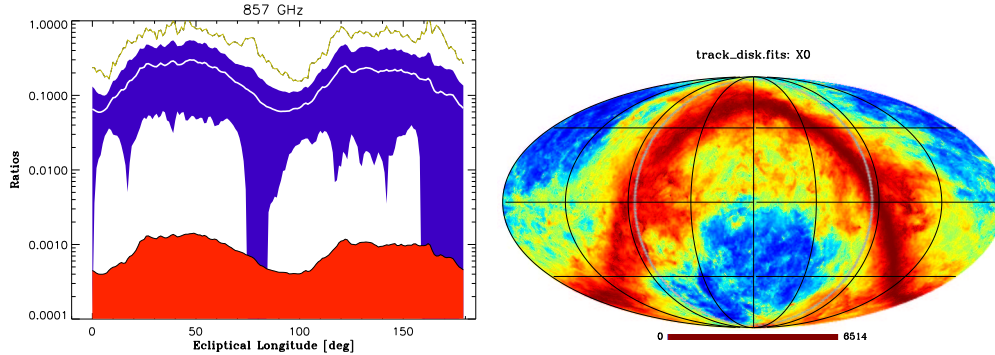


Fig. 1. Left frame: relative averaged contribution of ZLE and noise compared to the averaged Galaxy and computed over circular bands at 857 GHz. The ratio $I_{\text{ZLE}}/I_{\text{Galaxy}}$ for samples collected inside a circular band with given ecliptical longitude is reported. The ratio $I_{\text{noise}}/I_{\text{Galaxy}}$ is also reported. The white full-line is the average over the band, the blue the RMS, yellow the maximum ratio. In red the 1σ RMS of $I_{\text{noise}}/I_{\text{Galaxy}}$. Right frame: an example of scan band (gray) in the sky overlapped to a map of the Galaxy in ecliptical coordinates.

tical longitudes defined by the abscissa in the plot. The ratios $I_{\text{ZLE}}/I_{\text{Galaxy}}$ and $I_{\text{noise}}/I_{\text{Galaxy}}$ for the sky regions within the bands are computed. The noise refers here to a 14 month mission (2 sky surveys). It is evident that, despite the ZLE is generally subdominant compared to the Galaxy (the averaged ratios are 10 - 50 % of the Galaxy), its signal is well above the instrumental noise. Similar results are obtained also at lower frequencies since at large scale the spectral indices of Galaxy and the ZLE are comparable.

3. Perspectives from PLANCK

Current information does not allow to reach an accuracy better than $\approx 20\%$ in the ZLE modelling and removal; this is due in particular to the uncertainties on E_f below 1 THz. New, direct measures are needed to improve the situation. The ability of PLANCK to detect the ZLE signal improving the accuracy in E_f determination has been recently analysed (Maris et al. , 2006a) assuming that the COBE model properly represents the spatial distribution of the ZLE leaving as a free parameter E_f . Two methods have been considered. The first is based on the comparison of a template map for the Galactic emission with a spatial template for the ZLE calculated for given mission orbit

and scanning strategy. The second method is based on the comparison of observations of the same regions of sky taken at different epochs then exploiting the seasonal dependence in the ZLE observation. In both cases, since the ZLE varies over scales of $\approx 10^\circ$, one can consider template maps and observations at resolutions of $\approx 1^\circ - 2^\circ$ (this alleviates also the impact of possible local features, as those introduced by a non-perfect subtraction of point sources or by regions with peculiar frequency dependencies).

In these kinds of analysis, it is important to apply cuts to the data excluding regions where the Galaxy is very bright. Tab. 1 reports the relative error in the determination of E_f at the three highest PLANCK frequencies. The instrumental noise introduces (1σ) uncertainties below the 3% level in the worst case. Among the most relevant systematic effects, the relative calibration uncertainty is the dominant source of error. For a relative calibration RMS error of $\sim 1\%$ (0.1%) on patches of 2° radius, we find an absolute RMS error on E_f of $\sim 0.01 - 0.04$ ($\sim 0.001 - 0.004$) with only a weak dependence on the frequency in the range $\sim 300 - 900$ GHz, corresponding to relative errors on $E_f \sim 4\%, 10\%, 23\%$ ($\sim 0.4\%, 1\%, 2\%$), respectively at 857 GHz, 545 GHz, 353 GHz for

	Frequency Channel		
	857 GHz	545 GHz	353 GHz
Instrumental Noise	0.2%	0.8%	2.4%
Pointing (RMS 1 arcmin)	0.02%	0.03%	0.1%
Calibration (RMS 1%)	4%	10%	23%
Calibration (RMS 0.1%)	0.4%	1%	2%

Table 1. Estimated budget of relative error (1σ) for the determination of E_f in three frequency channels of PLANCK. Data are aggregated in independent circular patches with radius 2° . Reference E_f expect from the extrapolation described in the text are 0.6, 0.3 and 0.1 respectively for 857 GHz, 545 GHz, 353 GHz. Two hypotheses are provided for the calibration error.

the most likely E_f values expected on the basis of COBE/FIRAS data. Therefore, relative calibration could ultimately determine the final accuracy in the ZLE extraction from PLANCK data; the same likely holds also for other future surveys with collecting area larger than that of the PLANCK telescope.

4. Future developments

A new method, presently under study, to detect and measure the ZLE consists in pixelizing the sky according to some suitable scheme and then to generate sky maps by simply taking the “moments” of observations whose pointing directions are projected in the same sky pixel. This is a generalisation of what already done in composing maps from CMB surveys, where only “averages” of data are taken. In this framework, we plan to generate also maps of higher order moments which are sensitive to the variation of ZLE, due to the motion of the observer in the IDPs cloud during the survey, but not to the static Galactic and extragalactic background. Even in this case the pattern of higher order moments in the sky can be easily derived from 3D models of the IDPs distribution once the details of the orbit and scanning strategy of the observer are given and can be discriminated from the pattern induced by the instrumental noise or by the calibration errors. This approach has the advantage to allow to use all the samples acquired during the survey, instead of considering only those taken when the surveyor is at antipodal positions on its orbit. Moreover, “maps” of time series for

each pixel in the sky could be produced as well, each pixel being considered as a sort of “sensor” activated each time the scanning strategy leads the instrument to observe the corresponding sky region. Neural networks could be used to analyse this “time-series map”. We plan to study also the ability of PLANCK to improve even the geometrical parameters of the COBE model, to treat the case of large scale spatial dependencies of E_f and to identify even the tiny secondary components as, possibly, the weaker emission from the cloud of dust expected from the collisional erosion of KBO population Backman et al. (1995).

A web-site useful to distribute the products of these simulations to the whole community is in preparation.

Acknowledgements. The participation at this conference has been supported by INAF and ASI in the framework of the PLANCK mission Working Group 7, grant ASI/CRAM 2.15.020202 assigned to Catania, Trieste and Padua astronomical observatories; we warmly thank G. Umana for the authorization of the financial support.

References

- Ábrahám, P., Leinert, C., Lemke, D., 1997 A&A, 328, 702
 Backman, D.E., Dasgupta, A., Stencel, R.E., 1995, ApJ, 450, L35
 Bernstein, R.A., Freedman, W.L., Madore, B.F., — 2002a, ApJ, 571, 56; — 2002b, ApJ, 571, 85
 Bock, J., Battle, J., Cooray, A., et al. 2006, New Astronomy Reviews, 50, 215

- Bohren, C.F., Huffman, D. R., 1998, *Absorption and Scattering of Light by Small Particles* John Wiley & Sons, ISBN: 0471293407, New York, USA
- Cremonese, G., Marzari, F., Burigana, C., Maris, M., 2002, *New Astronomy*, (7/8), 483
- Dikarev, V., Grün, E., Baggaley, J., et al. 2005, *Adv. in Space Research*, 35, 1282
- Fixsen, D.J., Dwek, E., 2002, *Ap.J.*, 578, 1009
- Gor'kavyi, N.N, Ozernoy, L.M., Mather, J.C., 1997, *Ap.J.*, 474, 496
- Ishimoto, H., 2000, *A&A*, 362, 1158
- Kelsall, T., Weiland, J.T., Franz, B.A., Reach, W.T., Arendt, R.G., et al., 1998, *ApJ*, 508, 44 (also astro-ph/9806250)
- Maris, M., Burigana, C., Cremonese, G., Marzari, F., Fogliani, S., et al., 2003, Proc. of the *XLVII National Conference of the Italian Astronomical Society*, Mem.S.A.It. Suppl., 3, 318
- Maris, M., Burigana, C., Cremonese, G., Marzari, F., Fogliani, S., 2004, Proc. of the *Planetary Science: Fifth Italian Meeting*, 15 - 19 Sep. 2003, Gallipoli, Lecce, Italy, Eds. Blanco, A., Dotto, E., Orofino, V., p. 63
- Maris, M., Burigana, C., Fogliani, S., 2006a, *A&A*, 452, 685 (also astro-ph/0603048)
- Maris, M., Burigana, C., Fogliani, S., 2006b, Proc. of *CMB and Physics of the Early Universe*, 20 - 22 April 2006, Ischia, Italy, EU - Proceedings of Science, PoS(CMB2006)044 at <http://pos.sissa.it> (also astro-ph/0607439)
- Mattila, K, 2003, *ApJ*, 591, 119
- Reach, W.T., Abergel, A., Boulanger, F., Desert, F.-X., Perault, M., et al., 1996, *A&A*, 315, L381
- Reach, W.T., 1997, Proc. *Diffuse Infrared Radiation and the IRTS*, ASP Conf. Series, H. Okuda, T. Matamoto, T. Rollig eds Vol. 124, 33
- Reach, W.T., Morris, P., Boulanger, F., Okumura, K., 2003, *Icarus*, 164, 384
- Waller, W.H., Marsh, M., Bohlin, R.C., et al., 1995, *ApJ*, 110, 1255
- Wheelock, S.L., Gautier, T.N., Chillemi, J., Kester, D., McCallon, H., et al., 1994, *IRAS Sky Survey Atlas Explanatory Supplement*, JPL Publ. 94-11